RSC Advances

Preparation of Imatinib Base loaded Human Serum Albumin for Application in Treatment of Glioblastoma

Morteza Kamali[1], Rassoul Dinarvand[2], Hassan Maleki[1], Hossein Arzani[1], Parvin Mahdaviani[3],Houra Nekounam[1], Mahdi Adabi[1], Masood Khosravani[1]*

[1]*Department of Medical Nanotechnology, School of Advanced Technologies in Medicine, Tehran University of Medical Sciences, Tehran, Iran*

[2] *Department of Pharmaceutics, Faculty of Pharmacy, Tehran University of Medical Sciences, Tehran, Iran*

[3]*Nanomedicine and biomaterial Lab,Department of pharmaceutics,Faculty of pharmacy, Tehran University of Medical Sciences, Tehran, Iran*

*Corresponding Author Email: drkhosravani@tums.ac.ir

Tel: +98(0)21 88991118

Fax: +98(0)21 8899 1117

1

Abstract

Imatinib is a useful drug to inhibit some receptors such as c-kit and PDGFRs which are overexpressed in glioblastoma. However, Imatinib is easily effluxed by the proteins of the endothelial cells. The aim of this work was to synthesize imatinib base (IMTb) in nanoscale and also investigate the amount of its loading into the human serum albumin (HSA) nanoparticles. The desolvation method was used to synthesize the IMTb loaded HSA with the mean size about 80-90 nm. Fourier transform infrared spectroscopy (FT-IR) demonstrated that the non-covalent interactions between IMTb and HSA could not affect the chemical structure of IMTb. Differential scanning calorimetry (DSC) analysis indicated the amorphous form of IMTb in the HSA nanoparticles. Moreover, the capacity of encapsulation efficiency and drug loading were found 98% and 6.9%, respectively. The obtained results also exhibited that IMTb loaded HSA and free IMTb in the concentration of 40 μg/ml had approximately 90% and 55% cytotoxicity effect on U87MG glioblastoma cells, respectively. Therefore, IMTb loaded HSA nanoparticles can be introduced as potential candidate for drug delivery in the treatment of glioblastoma.

Introduction

Glioblastoma multiforme (GBM), is the most common malignant brain tumor with an incidence of 2–3 cases per one-hundred people, leads to the death in the most patients approximately one year from the time of diagnosis in early stages.[1-3] The current treatments including surgery, chemotherapy and radiation therapy are limited owing to the tumor's biology and its location into the brain.[2] Unfortunately, the recent advancement in the chemotherapy of brain tumor has not been enough efficiency and has only enhanced several months instead of several years of life.[1] With the advancements of nanotechnology, new methods of chemotherapy are being translated into a new generation of signal transduction and cell cycle control. These drugs can selectively act and may enhance chemotherapy efficiency via access for brain cancers.

Protein kinases play an essential role in the intracellular signal-transduction pathways with controlling the cell functions such as proliferation, invasion, migration, adhesion, and apoptosis.[4] Platelet-derived growth factor (PDGF) is a ligand for receptors of tyrosine kinases to control cell growth and division with important roles in brain tumor development. In Glioblastoma (GBL), the distortions of PDGF/PDGFR signal-transduction pathway such as stimulation of autocrine and paracrine ligands and protein overexpression can occur. Hence, PDGRF signalling pathway can be used as a potential target for the anticancer therapy. [5-10]

Imatinib mesylate (STI571, Gleevec) is considered as a powerful drug to inhibit the Bcr-Abl, PDGFRα, PDGFRβ, c-Fms, and c-Kit tyrosine kinases[11,12] and is used for the treatment of chronic myelogenous leukemia(CML) and gastrointestinal stromal tumors(GIST) due to the effect of its inhibitory on Bcr-AblIt and c-Kit, respectively.[13,14] Imatinib hinders phosphate transfer of ATP to protein kinases, resulting in lack of phosphorylation and signal transduction.[15] However, there are various efflux transporters in blood-brain barrier and blood-cerebrospinal fluid barrier which efflux anticancer drugs, leads to decrease in the

therapeutic effects. In order to overcome this problem, nanoparticles can be used as effective delivery tools to enhance the tumoricidal activities of anti-cancer drugs. Such delivery systems are suggested due to their tumor-targeting abilities, internalization efficiencies and dominant multidrug resistance.[16,17]

HSA due to its non-toxic and non-immunogenic advantages is considered as an efficient nanoparticle carrier.[18] Albumin binds to the 60-kDa glycoprotein (gp60) receptor and enter into cells via transcytosis and accumulate in tumors.[19] Likewise, the uptake of albumin-based nanoparticles increases in solid tumors owing to enhanced permeability and retention effect which results from pathophysiology of tumor tissue, angiogenesis, hypervasculature, deficient vascular and insuffcient lymphatic drainage.[20,21] For example, Yadav et al. prepared the paclitaxil nanoparticles via nanoemulsification using human serum albumin as polymer.[22] They reported that paclitaxil loaded albumin nanoparticles enhance the targeted drug therapy and act efficiently for removing the side effects of the cremophor EL. Dries et al also evaluated the effect of doxorubicin-loaded HSA nanoparticles on cell viability UKF-NB3, IMR 32. Their results exhibited that the inhibition of cell growth of doxorubicin-loaded HSA can be better in comparison with a doxorubicin control solution.[23]

In this study, IMTb loaded HSA nanoparticles were prepared by desolvation method in different pH and the amount of encapsulation efficacy and drug loading was tested. Besides, cytotoxic effects of IMTb loaded HSA nanoparticles were evaluated on U87MG cells.

Experimental section

Materials and reagents

IMTb (purity >99%) was purchased from Tufigh daru pharmaceutical Co. Ltd., IRAN-Karaj. Albumin (albumin 20% and purity 96%) and glutaraldehyde(8%) were bought from Merck (Germany). Fetal bovine serum (FBS), trypsin, phosphate buffer solution (PBS) and penicillin/streptomycin were from Sigma-Aldrich (Germany). The U87MG cell line was

purchased from pastor's institute (Iran) and Cell-line was cultured according to supplier's instructions. All other reagents were bought from Sigma-Aldrich (Germany)

Preparation of IMTb-HAS NPs

IMTb-HSA nanoparticles were prepared using a desolvation method.[24,25] First, the injectable albumin were dialyzed against double distilled water (DDW) for 2 hours (dialysis bag with cut-off=12000) to remove preservatives and stabilizers. Then, dialyzed albumin solution containing 200 mg of HSA was dissolved in 2 ml of DDW and pH was adjusted to 10 by adding 0.1 M NaOH.

Second; 15 mg of IMTb was dissolved in acetone (8 mL) and added dropwise with a constant rate of 1 ml/min to albumin solution which was under constant magnetic stirring(rpm=500). The nanoparticles were hardened with 25% glutaraldehyde (1.56 μg/mg of protein) for 16 hours under constant magnetic stirring at room temperature. The organic solvents were then removed under reduced pressure by rotary vacuum evaporation and the albumin nanoparticles were purified by ultra-centrifugation (20,000 g, 10 min) and redispersed in DDW. Each redispersion step was performed in an ultrasonication bath for 10 minutes. The sample was finally lyophilized at $-70\ ^{\circ}$C for 24 hours (Freeze Dry Telstar-spain). Albumin nanoparticles without drug loaded were prepared with the same approach.

Characterization of IMTb-HSA nanoparticles

Particle size and zeta potential measurement

The mean particle size of the IMTb-HSA nanoparticles was measured via dynamic light scattering (DLS) method (Malvern Zetasizer ZEN 3600). The lyophilized nanoparticles were suspended in and diluted with DDW and measured at $25\ ^{\circ}$C with a scattering angle of 90°. The zeta potential was also measured by electrophoretic laser doppler anemometry using zeta potential analyzer (Malvern Zetasizer ZEN 3600) and the size distribution was determined by a polydispersity index (PI).

DSC analysis

The thermal behavior of IMTb, HSA, physical mixture of IMTb and HSA and IMTb loaded HSA nanoparticles was studied by DSC (Mettle Toledo DSC823,Switzerland). The heating rate and nitrogen purges were 10 K/min and 20 mL/min, respectively.

FT-IR analysis

FT-IR spectra were measured using FT-IR spectrophotometer (Nicolet, model Magna-IR spectrometer 550). About 10 mg of sample was mixed with 200 mg of KBr and compressed into a pellet using a hydraulic press. FT-IR spectra over the scanning range of 400–4000cm^{-1} were obtained .

Standard curve of IMTb

For drawing standard curve, a stock solution of IMTb (1 mg) was prepared in PBS and acetonitrile. Various concentrations (5, 10, 20, 30, 40 μg/ml) were then prepared from stock solution and UV absorption of samples was measured at 280 nm and repeated three times for each sample. The Standard curve was plotted the absorbance versus concentration as shown in Fig. 1.

Fig. 1

Determination of drug Encapsulation efficiency and Drug loading

1 mg of IMTb loaded HSA nanoparticles was dissolved in 10 ml of acetonitrile and PBS and sonicated for 30 min for extracting IMTb. The amount of IMTb in the solution was measured by UV-visible (Optizeri 2120 UV plus). The results were compared with standard curve and extended to 10 ml supernatant and calculated by following equations:

$$\text{Efficacy encapsulation} = \frac{\text{the amount of IMTb for preparing nanoparticles} - \text{the amount of IMTb in supernatant}}{\text{the amount of IMTb for preparing nanoparticles}} \times 100$$

$$\text{Drug loading} = \frac{\text{the amount of IMTb for preparing nanoparticles} - \text{the amount of IMTb in supernatant}}{\text{the amount of IMTb for preparing nanoparticles} + \text{HSA weight}} \times 100$$

6

Encapsulation efficiency is defined as the ratio of weight of drug encapsulated into a carrier system to the total drug added whereas drug loading is defined as the ratio of drug to the weight of total carrier system.[26]

Drug release profile of IMTb loaded HSA nanoparticles

For deteimining IMTb release from HSA, 10 mg of IMTb loaded HSA nanoparticles was dispersed in 10 ml phosphate-buffered saline (PBS; pH 7.4). This solution was then enclosed in a dialysis bag and submerged in 100 ml PBS at 37 ◦C under steady shaking rate of 100 rpm/min. In various time intervals, 2 ml of medium was withdrawn and same volume of fresh medium was added. Each sample was mixed with 1.5 ml of acetonitrile, vortexed for 3 min and centrifuged at 1500 rpm for 5 min. The obtained supernatant was characterized three times for each sample by UV-vis (Optizeri 2120 UV plus).

In vitro cytotoxicity

Cell culture

Dulbecco's modified Eagle's medium (DMEM) was used for culturing U87MG cells. 10% (v/v) FBS (fetal bovine serum), 100 units/ml penicillin and 100 μg/ml streptomycin were added to DMEM. This cell line were maintained in a CO2 atmosphere at 37 °C with 5% humidity. For dose-dependent cytotoxicity assays, 96-well plates with 1×10^4 cells/well were used to seed the cells. These cells were pre-incubated for 24 h. Afterwards, fresh serum and free DMEM was replaced with the old media and the certain amounts of HSA nanoparticles, IMTb and IMTb loaded HSA nanoparticles were added for 24, 48 and 72 hours. The cytotoxicities of HSA nanoparticles, IMTb and IMTb loaded HSA nanoparticles were determined using MTT assays.

MTT assay

The effects of IMTb loaded HSA nanoparticles on U87MG cell's proliferation and survival were determined in 96-well plates by MTT assay. 96-well plates containing cells (except

control group) were added the given concentrations of IMTb loaded HSA nanoparticles (5,10,15, 20, 30 ,40 μg /ml) and IMTb and then incubated for 24, 48 and 72 hours. Afterwards, MTT formazan solution to the wells was added and incubated for 4 hours and DMSO was then added to the wells and the absorbance was measured at wavelength of 630 nm with a microplate reader (Biotek 808 Elx).

Results and discussion

Characterization of IMTb loaded HSA nanoparticles using DLS

IMTb-HSA nanoparticles in pH of 8, 9 and 10 were prepared whereas other parameters were constant. DLS analysis demonstrated that the mean size of nanoparticles in pH of 8, 9, and 10 were 574, 228 and 82 nm, respectively, which indicated to decrease in nanoparticle size by enhancing pH from 8 to 10. Besides, the zeta potential of nanoparticles in pH of of 8, 9, and 10 were -0.05, +1.25 and -31.00 mV, respectively. The results indicated that the zeta potential for pH of 10 was enough good to stabilize nanoparticles against the agglomeration. Therefore, the prepration of nanoparticles was optimized at pH=10 due to smaller size of nanoparticles (Fig. 2a) and moderate zeta potential (from ±30 to ± 40 mV) in Fig. 2b and repeated for three times which indicated the same sizes. Likewise, the polydispersity index of nanoparticles in pH=10 was 0.2.

Fig. 2

Characterization of IMTb loaded HSA nanoparticles using FT-IR

FT-IR analysis was used to detect the interactions between IMTb and HSA. As shown in Fig. 3, the spectrum of IMTb powders (curve 1) exhibit at 1659, 3050 and 3435 cm^{-1} which are attributed to C=O, C-H and N-H groups, respectively. Curve 2 shows the spectra of HSA nanoparticles with amide bonds (amide I) at 1600-1700 cm^{-1} and 1548 cm^{-1}(amid II). Curve 3 are related to the spectra of physical mixture of HSA and IMTb which shows no interaction between two mixtures in comparison with spectra of IMTb and HSA. Curve 4 are related to

IMTb loaded HSA nanoparticles and the stretching band C=O is shifted from1657 to 1650 cm^{-1} which can be due to interactions between IMTb and HSA in the IMTb loaded HSA nanoparticles. Besides, N-H bond was not observed in spectra of IMTb loaded HSA nanoparticles.

Fig. 3

Investigation of pH effect on encapsulation efficiency and drug loaded

Drug loading and encapsulation efficiency are considered as important parameters to investigate the properties of nanoparticles. The results indicated that pH did not have significant effect on the encapsulation efficacy and drug loading by increasing pH from 8 to 10 (as shown in table 1). This may be attributed to three dimensional structure of HSA which remain without change by increasing pH from 8 to 10.

Table 1

Characterization of IMTb loaded HSA nanoparticles using DSC

as seen in Fig. 4a, the melting endothermal peak of bulk IMTb was recorded at 100 °C and 215 °C and endothermal and exothermal peak of HSA nanoparticle was recorded at 100°C and 300 °C respectively (Fig. 4b). Three peaks at 100 °C, 215 °C and 300 °C are received as IMTb and HSA are mixed (Fig. 4c). However, in the IMTb loaded HSA nanoparticles, endothermal peak of IMTb at 215 °C was not detected and two peaks at 100 °C and 300 °C can be attributed to HSA (Fig. 4d). Therefore, it could be concluded that IMTb loaded in HSA nanoparticle change from crystal to amorphous or molecular state.[27]

Fig. 4

IMTb- loaded HSA release profiles in different incubation times

As shown in Fig. 5, release profile of IMTb loaded HSA nanoparticles were tested *in vitro* at 37 °C in PBS at pH 7.4 and compared with free IMTb (without HSA). The results exhibited that more than 80% of free IMTb was released in the first three hours of cumulative release

(from 7 to 80%) as seen in Fig.5a, whereas the release from HSA nanoparticles were 15, 37, 51, 58, 65 and 68% after 1, 6, 24, 48, 72 and 96 hours, respectively (Fig. 5b) which indicated fairly slow release profile and sustained release IMTb from HSA nanoparticles. The release results were similar to Aspirin loaded HSA nanoparticles which was investigated by Das et al. [28]

Fig. 5

Effect of IMTb loaded HSA on cell proliferation

The effects of IMTb and IMTb loaded HSA nanoparticles in concentrations of 5, 10,15, 20,30 and 40 μg/ml on the cell proliferation and survival of U87MG GBL cells were tested by MTT assay after incubating 24, 48, and 72 h. Fig. 6a shows the toxicity effect of free IMTb (without HSA) and IMTb loaded HSA nanoparticles on the cell proliferations and survival in different concentrations after 24 hours. Cell death due to toxicity of free IMTb for U87MG cells increased from 2 to 30% as the concentration of IMTb enhanced from 5 to 40% whereas cell death because of toxicity of released IMTb from HSA nanoparticles increased from 6 to 39% at the same concentrations for U87MG cells. Besides, cell death due to toxicity of released IMTb from HSA nanoparticles for U87MG cells is more after 48 and 72 hours. As seen in Fig. 5b and c, cell death owing to toxicity of free IMTb for U87MG cells increased from 0 and 17% to and 47 and 55%, respectively as the concentration of IMTb enhanced from 5 to 40% whereas cell death due to toxicity of released IMTb from HSA nanoparticles increased from 19 and 34% to 60 and 87% respectively, at the same concentrations for U87MG cells. The results also indicated that there are not any significant difference between free IMTb and IMTb-HSA in the toxicity rate as U87MG cells are exposed with free IMTb and IMTb loaded HSA for 24 hour whereas the toxicity rate of IMTb loaded HSA after exposing U87MG cells during 48 and 72 hours was 10% and 35% more than free IMTb, respectively which exhibit better efficacy of IMTb loaded HSA than free IMTb.

Fig. 6

Conclusion

Imatinib is introduced as a useful drug to inhibit some receptors which are overexpressed in glioblastoma. However, Imatinib is easily effluxed by the proteins of the endothelial cells, leads to decrease in the therapeutic effects of anticancer drugs. Nanoparticles are suggested due to their tumor-targeting abilities and internalization efficiencies. Our experiments indicated that albumin can play an effective role in fairly slow release profile of IMTb loaded HSA nanoparticles. The capacity of encapsulation efficiency and drug loading were found 98% and 6.9%, respectively. Moreover, cytotoxic effect of IMTb loaded HSA nanoparticles on U87MG cell line depends on concentration and time. In other words, the cytotoxicity effect enhance as concentration and their incubation time of IMTb loaded HSA nanoparticles increase and this cytotoxic effect of IMTb loaded HSA nanoparticles were higher than free IMTb for glioblastoma.

Acknowledgement

References

1 T. Kilic, J. A. Alberta, P. R. Zdunek, M. Acar, P. Iannarelli, T. O'Reilly, E. Buchdunger, P. M. Black, C. D. Stiles, Cancer Res., 2000, **60**, 5143.

2 M. L. Salgaller, L. M. Liau, Rev. Recent Clin. Trials, 2006, **3**, 265.

3 G. Kolata, L. K. Altman, Kennedy Case Shows Progress and Obstacles in Cancer Fight. New York Times, 2009.

4 L. N. Johnson, Q. Rev. Biophys., 2009, **19**, 1.

5 D. Hanahan, R. A. Weinberg, Cell, 2000, **100**, 57.

6 F. A. Al-Obeidi, K. S. Lam, Oncogene, 2000, **19**, 5548.

7 A. H. Shih, E. C. Holland, Cancer Lett., 2006, **232**, 139.

8 A. Guha, K. Dashner, P. L. M. Black, J. A. Wagner, C. D. Stiles, Int. J. Cancer, 1995, **60**, 68.

9 S. F. Johansson, Upsala J. Med. Sci., 2008, **113**, 1.

10 L. M. Strawn, E. Mann, S. S. Elliger, L. M. Chu, L. L. Germain, G. Niederfellner, A. Ullrich, L. K. Shawver, J. Biol. Chem., 1994, **33**: 21215.

11 E. Buchdunger, C. L. Cioffi, N. Law, D. Stover, S. Ohno-Jones, B. J. Druker, N. B. Lydon, J. Pharmacol. Exp. Ther., 2000, **295**, 139.

12 R. Capdeville, E. Buchdunger, J. Zimmerman, A. Matter, Nat. Rev. Drug Discov., 2002, **1**, 493.

13 B. J. Druker, M. Talpaz, D. J. Resta, R. N. Bin Peng, E. Buchdunger, J. M Ford, N. B. Lydon, H. Kantarjian, R. Capdeville, S. Ohno-Jones, C. L. Sawyers, N. Engl. J. Med., 2001, **344**, 1031.

14 G. D. Demetri, M. von Mehren, C. D. Blanke, A. D. Van den Abbeele, B. Eisenberg, P. J. S. L. Silberman, R. Capdeville, B. Kiese, B. Peng, S. Dimitrijevic, B. J. Druker, C. Corless, C.

D. M. Fletcher, H. Joensuu, N. Engl. J. Med., 2002, **347**: 472.

15 E. Buchdunger, T. O'Reilly, J. Wood, Eur. J. Cancer, 2002, **38**, 28.

16 J. D. Byrne, T. Betancourt, L. Brannon-Peppas, Adv. Drug Deliv. Rev., 2008, **60**, 1615.

17 J. Williams, R. Lansdown, R. Sweitzer, M. Romanowski, R. LaBell, R. Ramaswami, E. Unger, J. Controlled Release, 2003, **91**, 167.

18 W. Chen, B. Gu, H. Wang, J. Pan, W. Lu, H. Hou, Int. J. Pharm., **2008**, 362, 133.

19 N. Desai, V. Trieu, Z. Yao, L. Louie, S. Ci, A. Yang, C. Tao, T. De, B. Beals, D. Dykes, P. Noker, R. Yao, E. Labao, M. Hawkins, P. Soon-Shiong, Clin. Cancer Res., 2006, **12**, 1317.

20 T. A. John, S. M. Vogel, C. Tiruppathi, A. B. Malik, R. D. Minshall, Am. J. Physiol. Lung Cell Mol. Physiol., 2003, **284**: L187.

21 R. D. Minshall, C. Tiruppathi, S. M. Vogel, A. B. Malik, Histochem. Cell Biol. 2002, **117**, 105.

22 A. Anil Yadav, S. Vadali, Curr. Bioact. Compd., 2008, **4**, 51.

23 S. Dreis, F. Rothweiler, M. Michaelis, J. Cinatl Jr, J. Kreuter, K. Langer, Int. J. Pharm, 2007, **341**, 207.

24 S. Ko, S. Gunasekaran, J. Microencapsul. 2006, **23**, 887.

25 K. Langer, S. Balthasar, V. Vogel, N. Dinauer, H. von Briesen, D. Schubert, Int. J. Pharm., 2003, **257**: 169.

26 M. M. de Villiers, P. Aramwit, G.S. Kwon (Eds.), Nanotechnology in Drug Delivery (Biotechnology: Pharmaceutical Aspects), Springer, New York, NY (2009).

27 D. Q. M. Craig, M. Reading (Eds.), Thermal Analysis of Pharmaceuticals, CRC press (2007).

28 S. Das, R. Banerjee, J. Bellare, Trends Biomater. Artif. Organs, 2005, **18**, 203.

Figure Captions
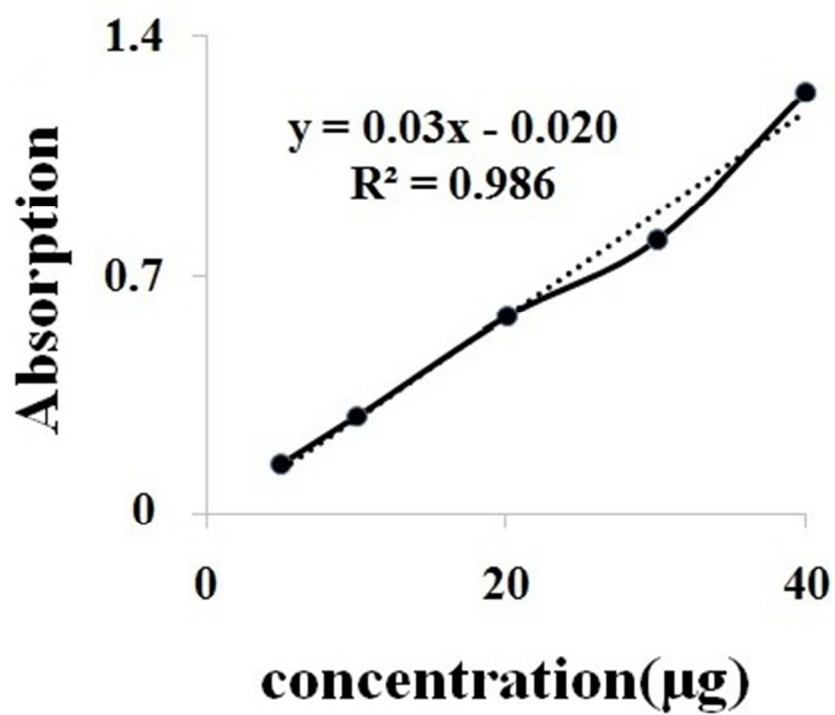
Fig. 1. Standard curve of imatinib base.

Fig. 2. Analysis of size and stability of synthesized IMTb-HSA nanoparticle in pH=10 by (a) DLS and (b) zeta potential.

Fig. 3. FT-IR spectra of (1) IMTb(black), (2) HSA(Mauve), (3) physical mixture of HSA/IMTb(Yellow) and (4) IMTb-HSA NPs (red).

Fig. 4. DSC of (a) IMTb, (b) HSA, (c) physical mixture of HSA/IMTb and (d) IMTb-HSA nanoparticles.

Fig. 5. Relese profile of (a) free IMTb (without HSA) and (b), IMTb-HSA nanoparticles.

Fig. 6. The cytotoxic effect of free drug and IMTb-HSA nanoparticles on U87MG cell lines after (a) 24, (b) 48 and (c) 72 hour.

Table 1. Effect of pH on encapsulation efficacy and drug loading

	pH 8	pH 9	pH 10
Encapsulation efficacy	98	98	98
Drug loading	6.8	6.9	6.9

Fig.1

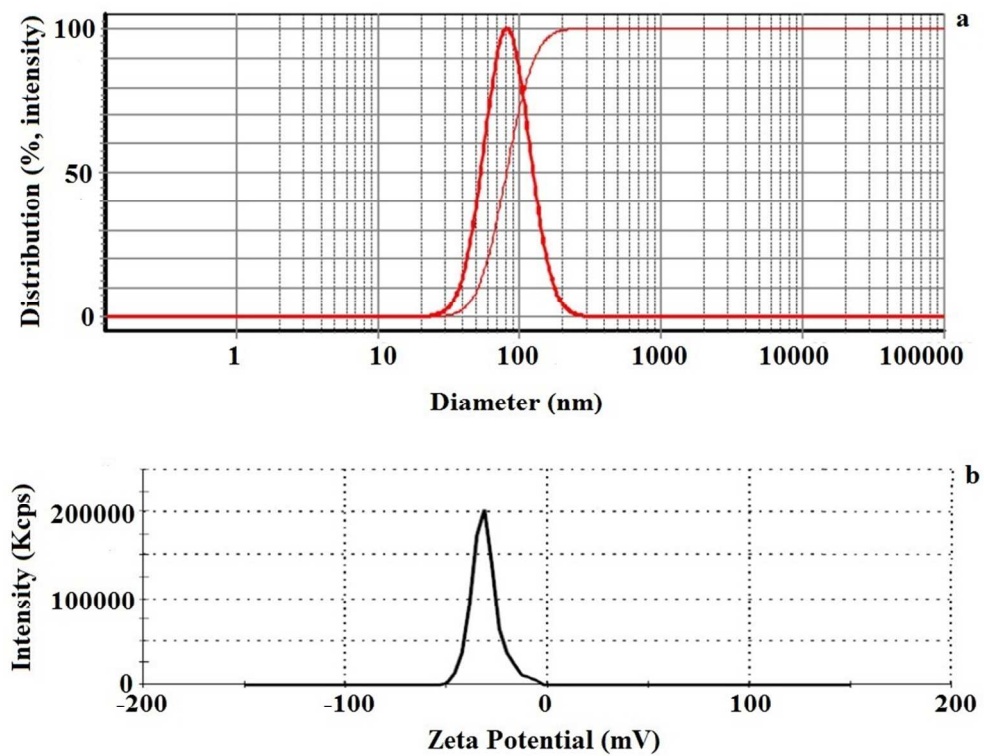Standard curve of imatinib base.
101x89mm (120 x 120 DPI)

Fig. 2

Analysis of size and stability of synthesized IMTb-HSA nanoparticle in pH=10 by (a) DLS and (b) zeta potential.
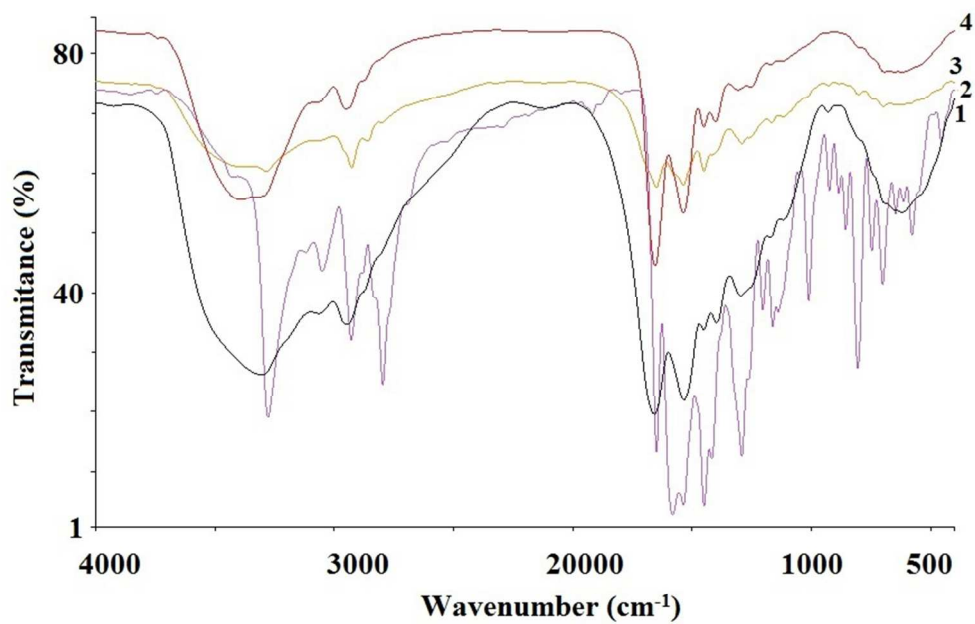209x169mm (120 x 120 DPI)

Fig. 3

FT-IR spectra of (1) IMTb(black), (2) HSA(Mauve), (3) physical mixture of HSA/IMTb(Yellow) and (4) IMTb-HSA NPs (red).
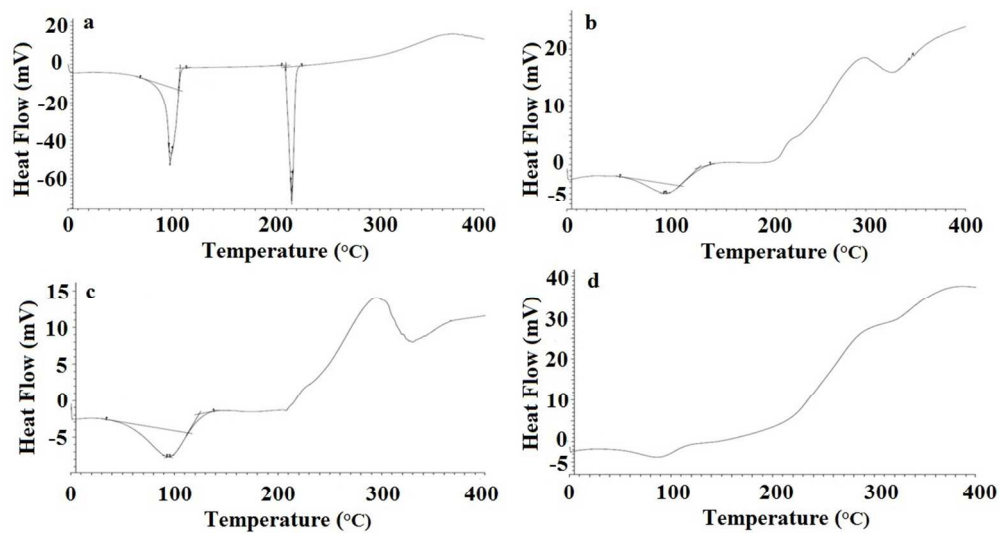189x131mm (120 x 120 DPI)

Fig. 4

DSC of (a) IMTb, (b) HSA, (c) physical mixture of HSA/IMTb and (d) IMTb-HSA nanoparticles.
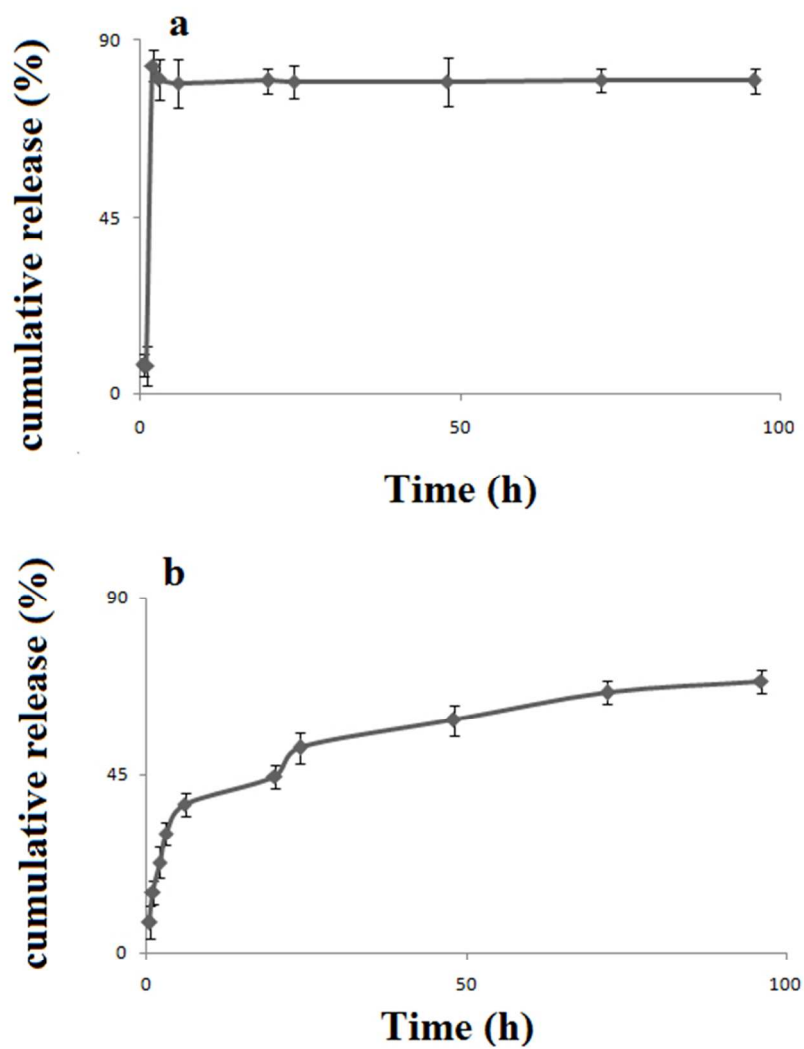256x148mm (120 x 120 DPI)

Fig. 5

Relese profile of (a) free IMTb (without HSA) and (b), IMTb-HSA nanoparticles
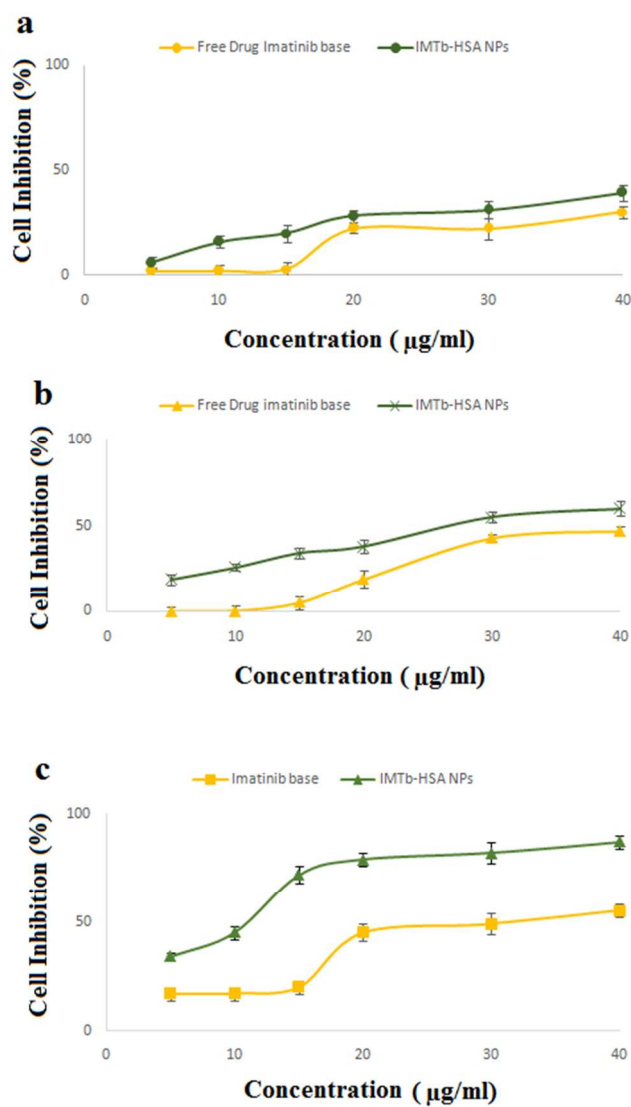115x164mm (120 x 120 DPI)

Fig. 6

The cytotoxic effect of free drug and IMTb-HSA nanoparticles on U87MG cell lines after (a) 24, (b) 48 and (c) 72 hour
111x192mm (120 x 120 DPI)